Lockett, R. D., Huang, Y. & Woolley, R. (2014). Instabilities in high pressure, iso-octane-air spherical explosion flames. Paper presented at the 8th International Seminar on Flame Structure, 21-24 Sep 2014, Berlin, Germany.

CITY UNIVERSITY LONDON

City Research Online

Instabilities in high pressure, iso-octane-air spherical explosion flames

Russel Lockett, Yue Huang

Department of Mechanical Engineering & Aeronautics,

The City University, London, EC1V 0HB

1. Abstract

High speed video shadowgraph and Schlieren images of spherical explosion flames obtained in the Leeds bomb have been analysed in the context of the Bechtold-Matalon linear model of spherical explosion flame instabilities. Analysis of the dispersion relation identifies the peninsula of instability, and the conditions for which the spherical explosion flame is conditionally and/or unconditionally unstable. Histograms of cellular length-scales have been derived, showing the change in cellular length scale with flame Peclet number. Non-linear effects result in larger wavenumber (small wavelength) cellularity than that predicted by the linear model. Finally, rich 3 bar and 4 bar explosion flames exhibit cellularity with two distinct ranges of wavenumber (wavelength) that may be linked to the Darrius-Landau hydrodynamic instability (small wavenumber instability), and the thermal-diffusive instability (large wavenumber instability).

2. Introduction

Thermal-diffusive effects present during the large flame stretch rate occurring in the early stages of expansion of a spherical explosion flame may temporarily stabilise the flame surface, until the underlying Darrius-Landau hydrodynamic instability causes the surface to become unstable [1]. The stabilisation or otherwise of the flame surface during expansion is dependent on the flame Lewis number (the ratio of the thermal diffusivity across the flame front to the molecular diffusivity of the deficient reactant in the preheat zone) and the Markstein number [2].

Bechtold and Matalon [3] have conducted a linear analysis of the stability of spherical explosion flames in which both hydrodynamic and thermal-diffusive effects are present. They derived a dispersion relation identifying the regime of stability and instability in terms of the solutions to a quartic equation involving the cellular wavenumber as a function of flame Peclet number (ratio of flame radius to laminar flame thickness), thermal diffusivity, Markstein number, and expansion ratio (ratio of unburned to burned gas density).

Any irregularity or disturbance on the flame surface will collapse or grow [3], defined by the relation

$$\mathrm{a} = \mathrm{a}_0 \mathrm{R}^{\omega(1+\varepsilon\Omega/\ln \mathrm{R})} \qquad 2.1$$

The rate of change of normalised disturbance amplitude is then

$$\frac{\mathrm{dA}}{\mathrm{dR}} = \frac{\omega \mathrm{A}}{\mathrm{R}}[1-\varepsilon(\mathrm{R})\Omega] \qquad 2.2$$

The transition from stability to instability is defined by the dispersion relation

$$Pe_{crit} = \frac{R}{\delta_l} = \Omega = \frac{Q_1 + lQ_2}{\omega} \qquad 2.3$$

where Q_1, Q_2, l and ω are defined by [4]

$$Q_1 = \frac{1}{(2a\omega+b-2a)}\left\{\frac{\ln\sigma}{\sigma-1}[(\sigma+1)n^4 + (2\omega+5)\sigma n^3 + (\omega\sigma - 2\sigma^2 + \sigma - 1)n^2 + (\sigma - 7 - 3\omega - \sigma\omega)n\sigma - 2\sigma(1+\omega)] + n(n^2-1)(n+2)\frac{(\sigma-1)}{\sigma}\right\} \qquad 2.4$$

$$Q_2 = \frac{1}{2\sigma(2a\omega+b-2a)}\,\alpha\{2n^4 + (2\omega\sigma + 2\omega + 10\sigma - 3)n^3 + (2\sigma\omega^2 + (5\sigma-1)\omega + 3\sigma - 2\sigma^2 - 2)n^2 + [\sigma\omega^2(1-4\sigma) - (14\sigma^2+1)\omega + 3 - 9\sigma - 8\sigma^2] \times n - 2\sigma(\omega^2 + 4\omega + 3)\} \qquad 2.5$$

$$l = \frac{2L_b}{\delta_L \alpha} + l_0,\ l_0 = \frac{-2\sigma\ln\sigma}{\alpha(\sigma-1)}, \qquad 2.6$$

$$\omega = \frac{-(b-a)+\sqrt{(b-a)^2-4ac}}{2a}, \qquad 2.7$$

where

$$a = n(\sigma + 1) + 1,\ b = 2n^2 + (4 + 5\,\sigma)n + 4, \qquad 2.8$$

and

$$c = -\frac{(\sigma-1)n^3}{\sigma} + 2n^2 + \left(3(\sigma + 1) - \frac{1}{\sigma}\right) n + 2. \qquad 2.9$$

The dispersion relation defining the regime of instability can be represented graphically by plotting cell wavenumber against Peclet number [4]. A typical graph of this form is displayed in Fig. 2.1 below.

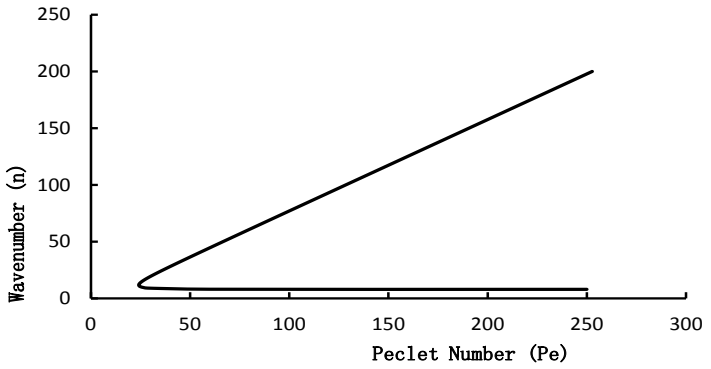

Fig. 2.1: Graph of cell wavenumber (n) versus Peclet number (Pe) for p = 2.0 bar, ϕ = 1.4 flame.

3. Approach

3.1 Experimental

High speed video shadowgraph imaging of spherical explosion flames at different conditions was obtained in the Leeds combustion bomb [5]. The windows of the bomb were 150 mm in diameter. A white light source was collimated using a large diameter convex lens, and the light was passed through the combustion vessel. The transmitted light was then focussed using a second convex lens 20 cm from the outlet window. The dynamically varying shadowgraph obtained from the spherical explosion flames were captured using a high speed video camera operating at 2000 fps.

3.2 Image Analysis

MATLAB was employed to determine the position and area of an extended selection of cells on the surfaces of a number of unstable explosion flames, from the onset of cellularity to later. The explosion flames analysed were: (1) p = 2.0 bar, ϕ = 1.4, (2) p = 2.0 bar, ϕ = 1.6, (3) p = 2.0 bar, ϕ = 1.8, (4) p = 2.0 bar, ϕ = 2.0 (5) p = 3.0 bar, ϕ = 1.4, (6) p = 4.0 bar, ϕ = 1.4.

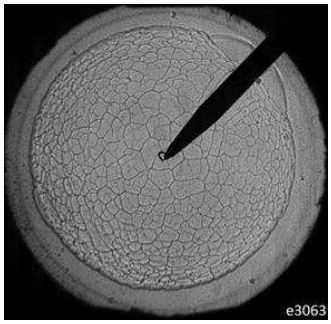

Figure 3.1(a) p = 2.0 bar, ϕ = 1.4

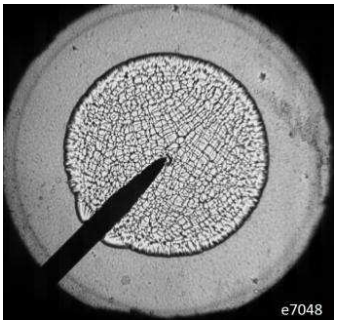

(b) p = 3.0 bar, ϕ = 1.4

(c) p = 4.0 bar, ϕ = 1.4

Sample flame shadowgraph images are presented in Figure 3.1 below. The images of the expanding explosion flames were employed to plot graphs of σS_L versus normalised flame stretch κ in order to derive the Markstein length and Markstein number.

Histograms of cell length scales and corresponding cell wavenumbers were derived from the cell areas during the expansion of the flame. This data has been added to the wavenumber-Peclet number stability curves in order to assess the limits of validity of the linear model. These are presented in the Results section.

3.3 Modelling

Chemkin was employed to model the laminar flame species and temperature profiles for all of the flames identified above, in order to obtain the laminar flame thickness and mean thermal diffusivity for each of the explosion flames.

4. Results and Discussion

Figure 4.1 shows a set of histograms of cell wavelengths, showing how the distribution of cell wavelengths vary as the flame expands, for the 2.0 bar, $\phi = 1.4$ explosion flame. Figure 4.1 shows that the mean cell wavelength decreases as the explosion flame expands. Figure 4.2 shows the cell wavenumbers derived from Figure 4.1 embedded in the stability curve of cell wavenumber versus Peclet number for this flame. The experimental cell wavenumbers shown in Figure 4.2 also demonstrate how the cells decrease in size with an increase in flame radius (Peclet number).

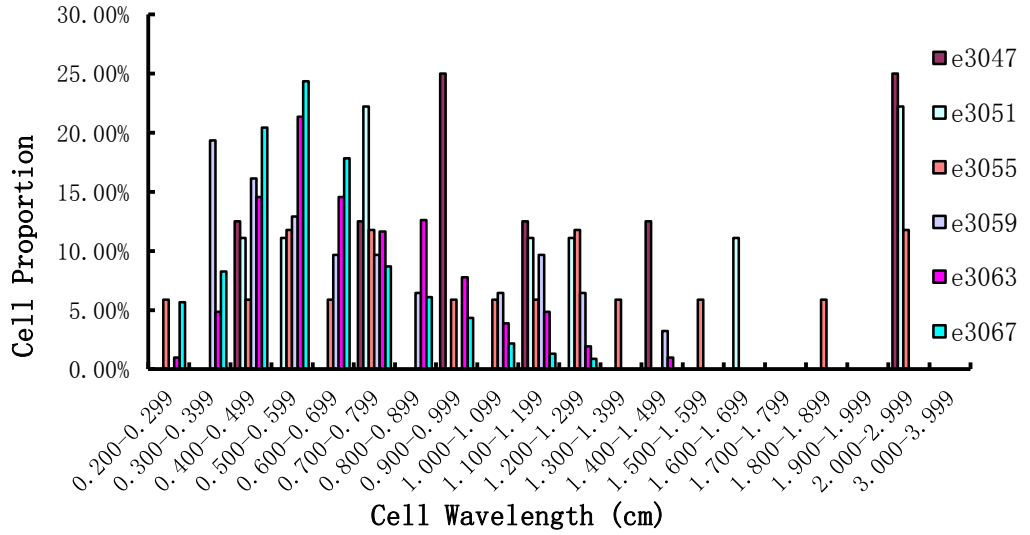

Figure 4.1: Histograms showing variation in cell wavelength as a function of flame expansion

Figure 4.2 shows that the linear theory predicts the onset of instability with reasonable accuracy. However, as the flame expands, non-linear effects result in an increase in cell wavenumber, significantly above that predicted by the linear model.

Figures 4.3 and 4.4 show the stability curves together with experimental data for the explosion flames identified in Figure 3.1 (b) and (c) respectively. Note that the theoretical stability curves in both graphs predict that both explosion flames are unconditionally unstable. The image of the 4.0 bar explosion flame shown in Figure 3.1 (c) shows cells containing two ranges of wavelengths; a short wavelength cellularity imbedded within a large wavelength cellularity. This dual wavenumber cellularity can also be seen in the cell wavenumber data included in Figure 4.3 (b).

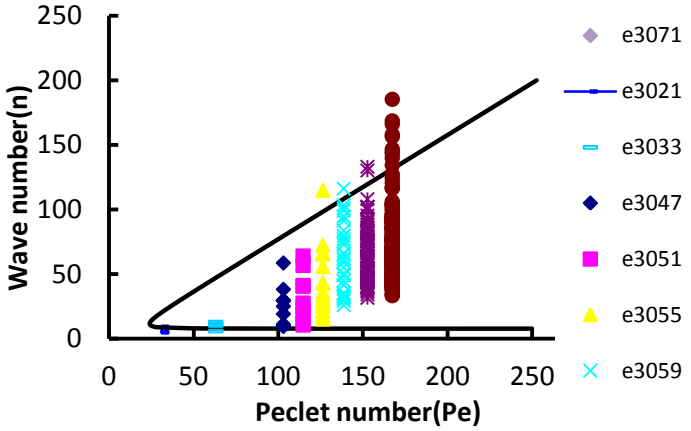

Figure 4.2: Stability curve of cell wavenumber versus Peclet number with experimental data.

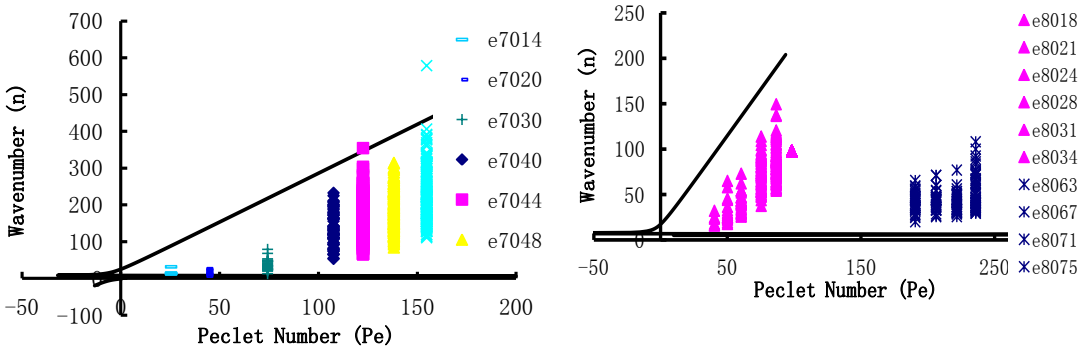

Figure 4.3 (a) Stability curve and wavenumber data for p = 3.0 bar, ϕ = 1.4 explosion flame.

(b) Stability curve and wavenumber data for p = 4.0 bar, ϕ = 1.4 explosion flame

5. Conclusions

The following conclusions can be drawn:

1. Mean cellular wavelengths are observed to decrease with flame radius.
2. Non-linear effects results in larger wavenumber cellularity than that predicted by the linear model.
3. The theoretical stability curves predict unconditional instability for ϕ = 1.4, 3.0 bar and 4.0 bar explosion flames.
4. A dual wavelength (wavenumber) cellularity is observed in the ϕ = 1.4, 4.0 bar explosion flame.

6. Acknowledgements

The authors would like to acknowledge the support of Dr R. Woolley (Univ. of Sheffield), who conducted the shadowgraph imaging experiments and Prof. C. Sheppard (Univ. of Leeds), who facilitated them.

7. References

1. D. Bradley, C.G.W. Sheppard, R. Woolley, D.A. Greenhalgh, R.D. Lockett, The Development and Structure of Flame Instabilities and Cellularity at Low Markstein Numbers in Explosions, Combust. Flame 122 (2000) 195 - 209.
2. D. Bradley, C.M. Harper; The development of instabilities in laminar explosion flames, 25'th Symp. (Int.) on Comb., The Combustion Institute 1994.
3. Bechtold, J. K., and Matalon, M., Hydrodynamic and Diffusion Effects on the Stability of Spherically Expanding Flames, Combust. Flame 67 (1987) 77 - 86.
4. D. Bradley, Instabilities and flame speeds in large-scale premixed gaseous explosions, Phil. Trans. Roy. Soc. A 357:1764 (1999) 3567 - 3581.
5. R. Woolley, C. Sheppard, unpublished data, University of Leeds (2007).